An Error and Sensitivity Analysis of the Atmospheric- and Soil-Correcting Variants of the NDVI for the MODIS-EOS

Alfredo R. Huete, *Member, IEEE,* and Hui Qing Liu

Abstract—**Several soil- and atmospheric-correcting variants of the normalized difference vegetation index (NDVI) have been proposed to improve the accuracy in estimating biophysical plant parameters. In this study, a sensitivity analysis, utilizing simulated model data, was conducted on the NDVI and variants by analyzing the atmospheric- and soil-perturbed responses as a continuous function of leaf area index. Percent relative error and vegetation equivalent "noise" (VEN) were calculated for soil and atmospheric influences, separately and combined. The NDVI variants included the soil-adjusted vegetation index (SAVI), the atmospherically resistant vegetation index (ARVI), the soil-adjusted and atmospherically resistant vegetation index (SARVI), the modified SAVI (MSAVI), and modified SARVI (MSARVI).**

Soil and atmospheric error were of similar magnitudes, but varied with the vegetation index. All new variants outperformed the NDVI. The atmospherically resistant versions minimized atmospheric noise, but enhanced soil noise, while the soil adjusted variants minimized soil noise, but remained sensitive to the atmosphere. The SARVI, which had both a soil and atmosphere calibration term, performed the best with a relative error of 10 percent and VEN of ±0.33 LAI. By contrast, the NDVI had a relative error of 20 percent and VEN of ±0.97 LAI.

I. Introduction

THE usefulness of the normalized difference vegetation index

$$\text{NDVI} = (\rho_{\text{nir}} - \rho_{\text{red}})/(\rho_{\text{nir}} + \rho_{\text{red}}) \quad (1)$$

for satellite assessment and monitoring of the Earth's vegetative cover has been demonstrated now for over a decade [1], [2]. The integral and time series analyses of seasonal NDVI data have provided a method of estimating net primary production over varying biome types, of monitoring phenologic patterns of the earth's vegetative surface, and of assessing the length of the growing season and dry-down periods, which are helpful in remote sensing studies of ecosystem structure and function, land cover classification, and carbon and biogeochemistry cycles of the earth [3], [4].

Manuscript received September 20, 1993; revised March 25, 1993. This was supported by MODIS under Contract NAS5-31364.

The authors are with the Department of Soil and Water Science, University of Arizona, Tucson, AZ 85721.

IEEE Log Number 9402671

The accuracy and precision of the NDVI is thus crucial for a large array of Earth Observation System (EOS) studies requiring knowledge of the state and dynamics of the Earth's vegetative cover. The validity of these "global" applications of the NDVI are based on several observational and simulated studies that have empirically related the NDVI to plant biophysical parameters, such as leaf area index (LAI), absorbed photosynthetically active radiation (APAR), percent cover, and biomass [5]–[8]. For globally based studies, however, we cannot assume that these regression relationships and statistical features will remain constant under changing atmospheric conditions and over spatially variable locations.

Many studies have found the NDVI to be unstable, varying with soil, sun-view geometry, atmospheric conditions, and the presence of dead material, as well as with changes within the canopy itself [8]–[11]. As a result, several studies and developments have sought to improve upon the NDVI by correcting for soil and atmospheric sources of variance.

The improved variants to the NDVI equation attempt to either incorporate a "soil" adjustment factor or a "blue" band for atmospheric normalization. The soil adjusted vegetation index (SAVI) introduced a soil calibration factor L to the NDVI equation to account for first-order soil–vegetation optical interactions and differential red and NIR extinction through the canopy [12]:

$$\text{SAVI} = [(\rho_{\text{nir}} - \rho_{\text{red}})/(\rho_{\text{nir}} + \rho_{\text{red}} + L)](1 + L). \quad (2)$$

An L value of 0.5 in reflectance space was found to minimize soil brightness variations and eliminated the need for additional calibration for different soils. The basis of the SAVI in minimizing the soil "noise" inherent in the NDVI has been corroborated in numerous studies involving ground, air, satellite, and simulated data sets [13]–[15].

Several refinements of the SAVI equation have also been investigated. Baret *et al.* [16] developed a soil-specific, transformed SAVI (TSAVI) utilizing SAIL model simulations. Using ground-based radiometric measurements over corn plots, Bausch [13] tested a step-wise variable L function in the SAVI but found no significant

improvement in soil noise reduction, although a greater dynamic range did occur. Qi *et al.* [17] developed a modified SAVI (MSAVI) that utilized an iterative, continuous L function to optimize soil-adjustment and increase the dynamic range of the SAVI:

$$\text{MSAVI} = \{2\rho_{\text{nir}} + 1 - [(2\rho_{\text{nir}} + 1)^2 - 8(\rho_{\text{nir}} - \rho_{\text{red}})]^{0.5}\}/2. \quad (3)$$

The atmospherically resistant vegetation index (ARVI), on the other hand, incorporated the blue band into the NDVI equation to normalize temporal and spatial variations in atmospheric aerosol content [18]:

$$\text{ARVI} = (\rho^*_{\text{nir}} - \rho^*_{rb})/(\rho^*_{\text{nir}} + \rho^*_{rb}) \quad (4)$$

where

$$\rho^*_{rb} = \rho^*_r - \gamma(\rho^*_b - \rho^*_r). \quad (4')$$

The ARVI utilizes the difference in the radiance between the blue channel and the red channel to correct the radiance in the red channel, and thus, reduce atmospheric influences. This index requires prior corrections for molecular scattering and ozone absorption ρ^*. Myneni and Asrar [19], in a sensitivity study with simulated data, found the ARVI to reduce atmospheric effects and to mimic ground-based NDVI data.

The NDVI variants (SAVI, MSAVI, and ARVI) either adjust for soil or atmosphere and do not consider combined interactive effects of soil and atmosphere. The ARVI only considers atmospheric noise without concern for soil noise and the SAVI and MSAVI do not consider atmospheric influences. However, one may integrate the L function in the SAVI with the blue-band normalization in the ARVI and derive the soil and atmospherically resistant vegetation index (SARVI) [18], which would correct for both soil and atmospheric noise, as would an MSARVI:

$$\text{SARVI} = [(\rho^*_{\text{nir}} - \rho^*_{rb})/(\rho^*_{\text{nir}} + \rho^*_{rb} + L)](1 + L) \quad (5)$$

and

$$\text{MSARVI} = \{2\rho^*_{\text{nir}} + 1 - [(2\rho^*_{\text{nir}} + 1)^2 - 8(\rho^*_{\text{nir}} - \rho_{rb})]^{0.5}\}/2. \quad (6)$$

The moderate resolution imaging spectrometer (MODIS), being developed for EOS, has several characteristics of interest to global vegetation index studies [20], [21], including an absolute radiometric accuracy of less than 5 percent ($\lambda \leq 3$ μm), improved spectral stability requirements, narrower spectral bandwidths, and band-to-band registration requirements of less than 0.2 IFOV, with 0.1 IFOV as a goal (Table I). Improved vegetation sensitivity will also be achieved from an optimal utilization of the 36 MODIS spectral bands between 0.415 and 14.235 μm with spatial resolutions of 250 m (two bands), 500 m (five bands), and 1000 m (29 bands). There is a near-infrared band (0.841–0.876 μm) that avoids the water absorption regions in the NIR and there is a "blue" band (0.459–0.479 μm) for implementation of the atmospherically resistant VI's (Table I).

TABLE I
MODIS SENSOR CHARACTERISTICS IN SUPPORT OF THE VEGETATION INDEX ALGORITHM PRODUCTS

Band #	Center Wavelength, λ_c (nm)	$\Delta\lambda$ (nm)	Ground IFOV (m)	Max. Spectral Radiance[1]	Required SNR[2]	Bandwidth Tolerance (±nm)
1	645	50	250	21.8	128	4.0
2	858	35	250	24.7	201	4.3
3	469	20	500	35.3	243	2.8
4	555	20	500	29.0	228	3.3
5	1240	20	500	5.4	74	7.4
6	1620	24.6	500	7.3	275	9.8
7	2130	50	500	1.0	110	12.8

[1]Watts/meter^2/micrometer/steradian.
[2]Signal-to-noise ratio.
Quantization: 12 b.
Scan width: 2330 × 10 km (track) at 705 km platform altitude ±55° along scan.
Absolute calibration: ±5 percent, ± 2 percent reflectance.
Spectral Stability: λ_c and $\Delta\lambda$ stable to <2 nm (visible: desired for NIR).
Band-to-band registration: ±0.2 IFOV, with ±0.1 IFOV goal.

In this paper, a sensitivity analysis was performed on the NDVI and variants (SAVI, MSAVI, ARVI, SARVI, and MSARVI) using SAIL model simulations [22] over a range of LAI and soil background conditions. The analysis included a Lowtran atmospheric simulation [23] over a range of visibilities, with and without a Rayleigh component and ozone absorption. The purpose was to determine which NDVI variants were most appropriate for global vegetation studies with the MODIS sensor and to determine the accuracy or uncertainty with which one may estimate vegetation "changes" or "differences" utilizing these indexes.

II. Error and Sensitivity Analysis

The sensitivity approach utilized here is based on plotting a perturbed response of the VI as a continuous function of a vegetation biophysical parameter, such as the LAI [24]. The perturbation variables included soil brightness/wetness, atmospheric aerosol loadings, and molecular scattering/absorption. The percent relative error was used as a basis for comparing differences among VI's, and is defined as

$$\epsilon_r \text{ (percent)} = 100 \times (\text{VI}_p - \text{VI})/(\text{VI} - \text{VI}_s) \quad (7)$$

where VI is the "true" VI value (here the mean VI is treated as the true VI), VI_p is the perturbed VI response resulting from a change in the soil background and atmosphere, and VI_s is the VI response over bare soil (the lower boundary condition for the VI dynamic range). The percent relative error standardizes the unique dynamic ranges of the VI's. A second measure of VI performance is the "vegetation equivalent noise":

$$\text{VEN} = (\text{VI}_p - \text{VI})/\delta(\text{LAI}) \quad (8)$$

where δ (LAI) is the slope, $dVI/dLAI$, of the VI–LAI curve at a specific LAI. The VEN measures the uncertainty in estimating a vegetation parameter and carries the units of that parameter, e.g., LAI [24].

The VI error and sensitivity analyses were applied to nine cases:

1) the soil noise problem with no atmosphere (total atmospheric correction scenario);
2) the atmospheric noise problem with constant (mean) soil background (no soil variation);
3) the atmospheric noise problem over different soil backgrounds;
4) the soil noise problem for different atmospheres;
5) the combined or total soil and atmospheric noise;
6) the combined noise with and without a Rayleigh and ozone correction;
7) instrument noise associated with an absolute radiometric uncertainty of $\pm$ 5 percent;
8) instrument noise associated with a band-to-band registration (cross- and along-track directions) uncertainty of $\pm$ 20 percent and;
9) instrument noise associated with a spectral stability uncertainty of $\pm$ 2 nm.

The first case permitted an assessment of the impact of the total atmospheric (including aerosols) correction on the noise and uncertainty levels in the VI's. With the sixth case, we were able to compare partially corrected (Rayleigh and ozone) results with uncorrected and total atmospherically corrected VI's. The purpose of the last three cases was to compare atmospheric and soil noise with instrument-related uncertainties. The instrument error would define the lower threshold of VI noise and uncertainty from which the VI equation could not be further improved.

III. Data Set Description

A SAIL model simulation [22] was performed using a single-layer one-component canopy model with a uniform leaf angle distribution. The reflectance and transmittance properties of cedar tree leaves were used with canopy LAI values from 0 to 3 for a solar zenith angle of 40° and nadir view. Six soil backgrounds were used representing a reasonable range in soil optical properties, varying from 5 to 35 percent in red reflectances and 10 to 40 percent in the near-infrared (NIR).

A PC Lowtran atmospheric simulation [23] was conducted with a midlatitude summer, rural aerosol atmosphere model with visibilities of 5, 10, 23, 50, and 100 km, with and without a Rayleigh correction,

$$L_{(\text{Rayleigh corrected})} = (L_{(v)} - L_{(\text{Rayleigh})})/T_{(\text{Rayleigh})} \quad (9)$$

where $L_{(v)}$ is the measured radiance for any visibility, $L_{(\text{Rayleigh})}$ is the path radiance of the Rayleigh atmosphere, and $T_{(\text{Rayleigh})}$ is the one-way (vertical) transmission through the Rayleigh atmosphere. In both the SAIL and Lowtran model simulations, the fine spectral resolution data (10 nm) were averaged to approximate the MODIS bandpasses (Table I).

IV. Results

A. Total Atmospheric Correction (Soil Noise Only)

Fig. 1 shows the six vegetation index variants plotted against the LAI, utilizing six soil backgrounds from the model simulation. There were only soil "noise" perturbations with no atmosphere layer, equivalent to a "total atmospheric correction" scenario. A change in the soil background altered the red and NIR canopy reflectances and calculated VI's. For any constant level of green vegetation, these deviations were treated as "noise" and subjected to a sensitivity analysis as well as an error analysis. The atmospherically resistant VI's (ARVI, SARVI, and MSARVI) were included in these analyses despite the absence of an atmosphere to normalize. It was of interest to determine how the blue-band inclusion into the VI's would impact on soil noise.

Visually, there were higher soil influences in the NDVI and minimal soil noise in the soil-adjusting SAVI and MSAVI. The respective atmospheric resistant versions of these three indexes (ARVI, SARVI, and MSARVI) aggravated the soil noise problem.

The percent errors, due to soil noise, in the SAVI and MSAVI were the least at LAI's from 0 to 1, with those of the SARVI and MSARVI intermediate, and ARVI and NDVI the highest [Fig. 2(a)]. All indexes exhibited decreasing percent error due to soil with increasing LAI. At LAI's beyond 1.5, the percent relative error for all VI's became similar. The vegetation equivalent noise (VEN) values were also lowest for the SAVI and MSAVI at lower LAI's [Fig. 2(b)], where the uncertainty was within $\pm$ 0.05 LAI. The SARVI and MSARVI had the lowest VEN values from LAI 1.5 to 3.0 and all indexes had minimal noise levels at LAI = 3. The VEN values in the NDVI and ARVI were much higher and increased with LAI from 0 to 1.5 before decreasing again. The ARVI had the highest VEN with the greatest uncertainty ($\pm$0.5 LAI) at LAI = 1.5. At LAI values beyond 1.5, the VI–LAI curve (Fig. 1) started to level off, resulting in higher potentials for error estimates in LAI. At LAI = 3, soil influences disappear and the VEN levels drop to zero.

B. Atmospheric Noise Component

For the atmospheric sensitivity analysis, we chose a "mean" soil background and only perturbed the VI with atmospheric variations, namely aerosol contents (visibilities) with the Rayleigh component removed. The six VI's showed that as atmospheric visibility decreased, the VI response decreased with greater absolute changes occurring at the higher LAI's (Fig. 3). The atmospherically resistant VI's showed lower atmospheric variations than their nonatmospheric counterparts, with the ARVI resulting in the least variation. Thus, inclusion of the blue band into the VI equation (ARVI, SARVI, and MSARVI) resulted in improved normalization of atmospheric effects.

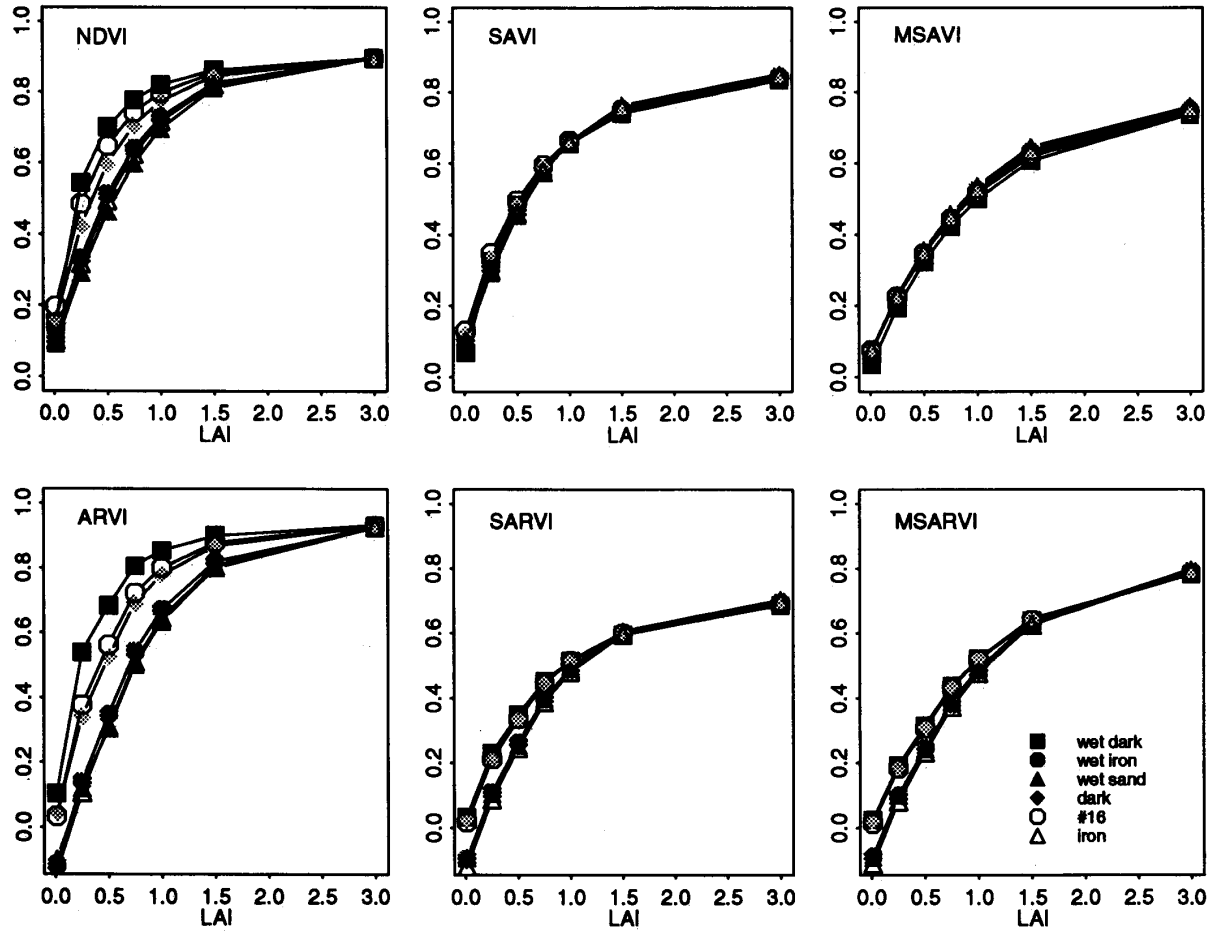

Fig. 1. Vegetation index response as a function of LAI for different soil backgrounds.

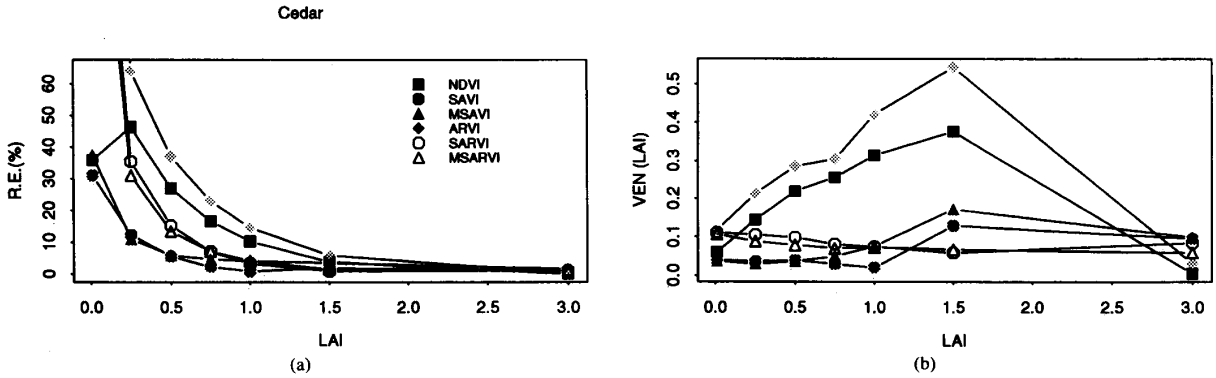

Fig. 2. Percent relative error (a) and vegetation equivalent noise (b) due to soil background as a function of LAI.

The lower error and noise levels of the atmospherically resistant indexes (ARVI, SARVI, and MSARVI) are seen in Fig. 4. The three self-atmosphere-correcting indexes had VEN levels below 0.7 LAI units, while the SAVI, MSAVI, and NDVI had VEN values approaching ± 1.5 LAI. In contrast to the soil case [Fig. 2(b)], all VI's increased in VEN with LAI, whereas the percent relative error was nearly independent of vegetation amount.

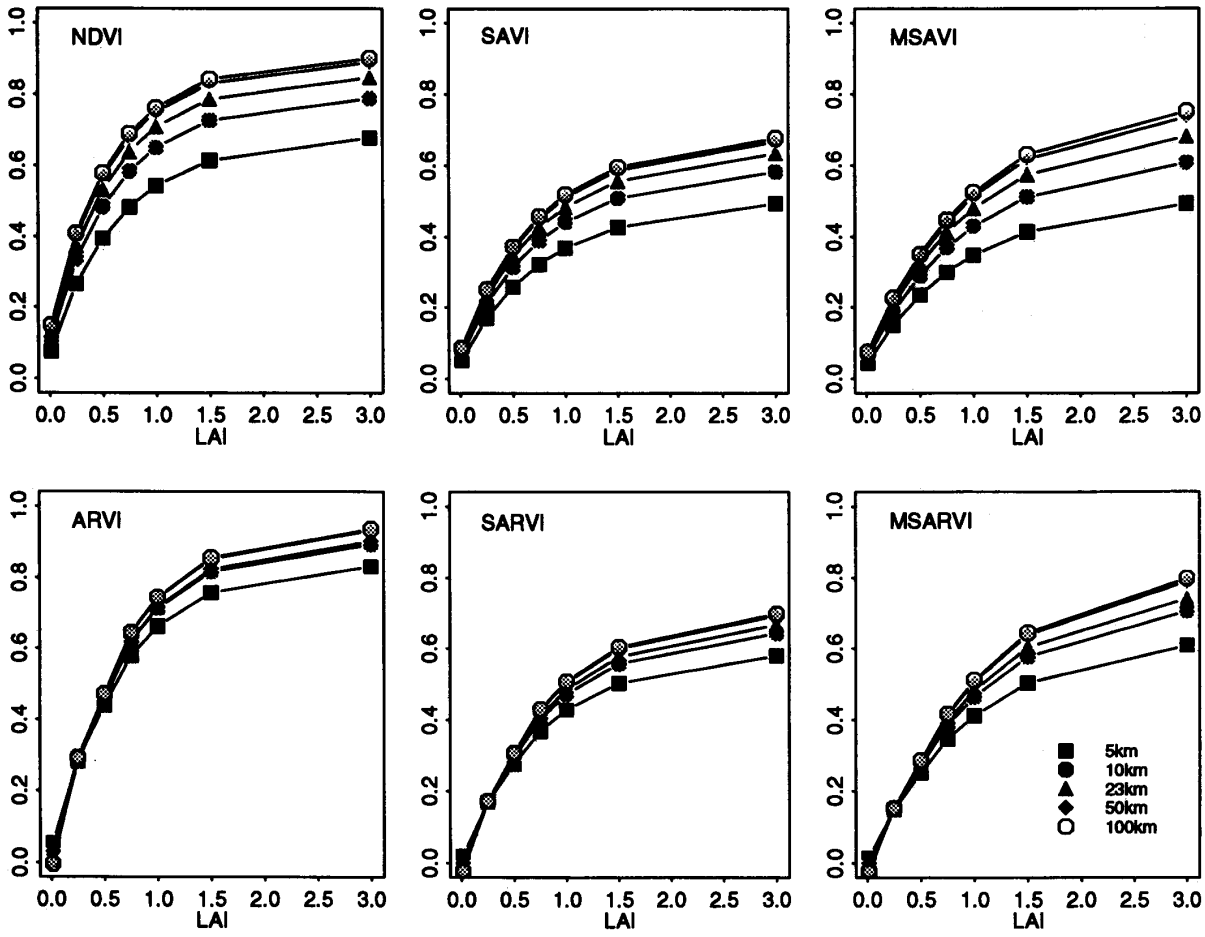

Fig. 3. Vegetation index response as a function of LAI for different atmospheric conditions.

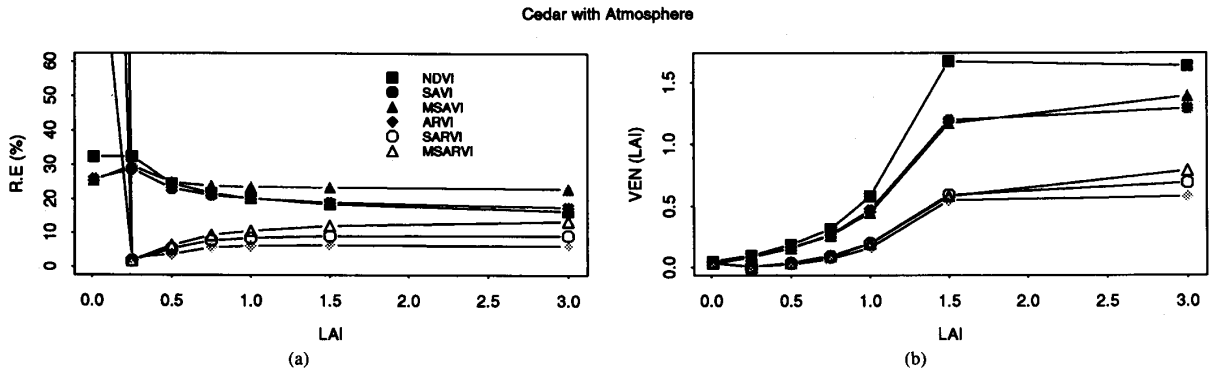

Fig. 4. Percent relative error (a) and vegetation equivalent noise (b) due to atmospheric influences as a function of LAI.

C. Coupled Atmospheric-Soil Noise

The atmosphere not only affected the vegetation signal but also the soil background signal. Thus, the error and uncertainty introduced by variable atmospheres, not only varied with the amount of vegetation, but also with the canopy background (Fig. 5). This analysis was similar to that presented in Fig. 4(b), but with a dark and bright soil background rather than the mean soil background. At-

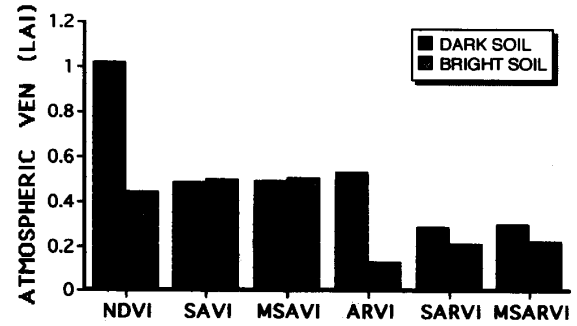

Fig. 5. Averaged vegetation equivalent noise due to atmosphere for a dark and a bright soil background.

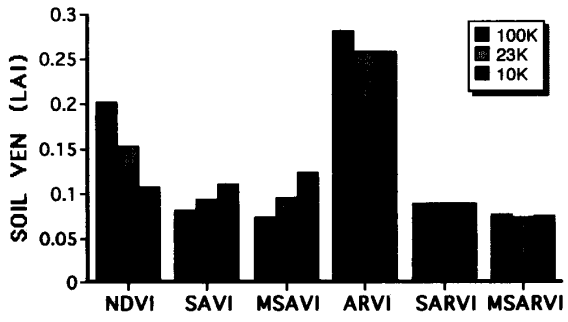

Fig. 6. Averaged vegetation equivalent noise due to soil background for 100 K, 23 K, and 10 K, Rayleigh corrected atmospheres.

mospheric noise was much more pronounced over canopies with darker soil backgrounds with the NDVI and ARVI, and less so in the SARVI and MSARVI. Atmospheric noise was nearly independent of soil background in the case of the SAVI and MSAVI (Fig. 5). Overall, the least noise resulting from atmospheric aerosols occurred with the atmospherically resistant variants and under conditions of low LAI's [Fig. 4(b)], and brighter soil backgrounds (Fig. 5).

D. Soil Noise with Varying Atmospheres

The interactive effects of soil and atmosphere also cause "soil" noise to not only vary with vegetation amount, but also atmospheric conditions (Fig. 6). Thus, the magnitude of soil noise in a VI may be positively or negatively reinforced by atmospheric aerosol contents. In Fig. 6, the soil noise in the NDVI decreased with higher aerosol loadings (lower visibilities), in contrast to the SAVI and MSAVI, which increased in soil noise under more turbid (aerosol) conditions.

Soil noise in the atmospherically resistant VI's (ARVI, SARVI, and MSARVI) was relatively stable across atmospheric conditions. The ARVI had the most soil noise, while the SARVI and MSARVI had the least soil noise. Under very turbid atmospheric conditions the NDVI had lower soil noise levels than found in the SAVI and MSAVI. Apparently, atmospheric turbidities dampened soil variations, and thus, atmospheric noise counteracted soil noise effects. Improved atmospheric correction algorithms would consequently enhance soil noise in the NDVI.

E. Total Noise

Both soil and atmospheric influences were allowed to simultaneously perturb the VI response, resulting in a soil-atmosphere (total) error and noise assessment of each VI as a continuous function of vegetation amount (Fig. 7). This represented the uncertainty in a VI when knowledge of atmospheric and soil optical parameters within an image are unavailable.

For most of the range of LAI's the "soil and atmosphere correcting" SARVI and MSARVI had the lowest

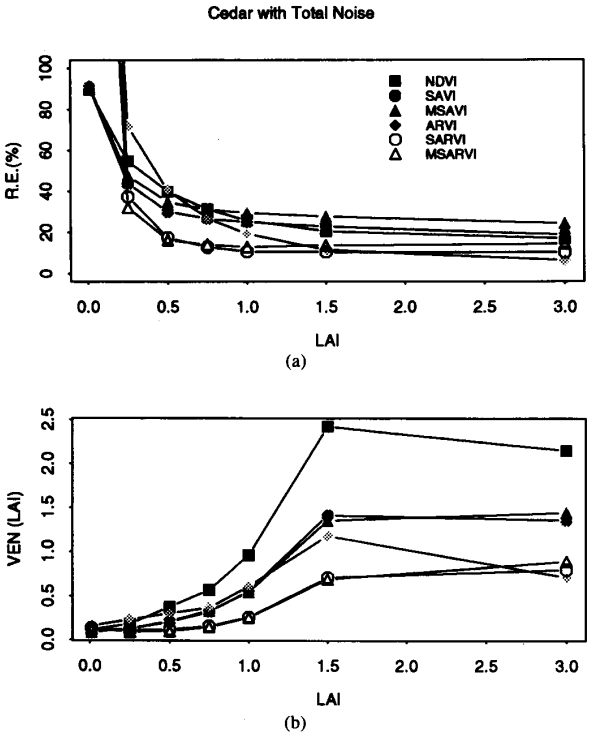

Fig. 7. Percent relative error (a) and vegetation equivalent noise (b) due to combined soil and atmospheric influences as a function of LAI.

percent relative error (~15 percent), while the NDVI, SAVI, and MSAVI had relative errors from 20 to 30 percent. The VEN values showed the NDVI to be least reliable in LAI estimation with uncertainties of ±2 LAI units at LAI levels beyond 1.5. By contrast, the SARVI and MSARVI could predict LAI to within ±0.75 throughout the range of LAI values (0–3). The ARVI, SAVI, and MSAVI were intermediate in behavior with LAI uncertainties leveling out at ±1.2.

Fig. 8 shows the effect of the Rayleigh component on combined atmospheric-soil (total) noise in all VI's. Overall, a Rayleigh and gas absorption correction improves upon vegetation sensitivity except in the case of the NDVI, where the gain in vegetation sensitivity is offset

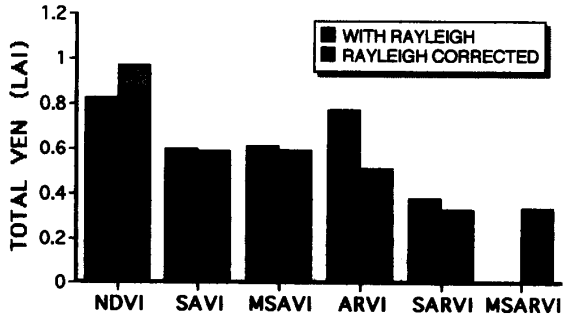

Fig. 8. Comparison of "total" (soil and aerosols) vegetation equivalent noise for Rayleigh and Rayleigh corrected atmospheres.

by a higher increase in soil noise. Rayleigh correction had little effect on noise levels in the SAVI and MSAVI. The noise in the atmospherically resistant VI's, however, improved with Rayleigh correction, particularly in the ARVI. The MSARVI could not be computed with the Rayleigh component due to negative values in the square root term [(6)].

Fig. 9(a) shows total VEN values for each VI, averaged across the range of LAI's. The VEN due to soils varied from ±0.06 LAI (SAVI) to ±0.27 LAI (ARVI). The VEN values due to atmosphere, were overall, higher than those attributed to soils, and were lowest for the ARVI and SARVI (±0.2 LAI) and highest for the NDVI (±0.65 LAI). The "total" VEN analysis resulted in the SARVI having the lowest noise (±0.33 LAI) for the range of atmospheric and soil conditions analyzed in this study. The highest noise was encountered with the NDVI (±0.97 LAI). All indexes had noise and error terms that were nearly additive, i.e., the VEN due to soil plus that due to atmosphere approximated the total VEN.

For comparison purposes, the VEN due to different instrument characteristics are also shown in Fig. 9(a). The largest source of instrument noise considered here was due to an absolute radiometric uncertainty of ±5 percent in MODIS bands 1, 2, and 3. This resulted in VEN levels of ± ~0.12 LAI, which was of the same order of magnitude as soil noise. The noise resulting from a 20 percent band-to-band registration error was relatively small (± ~0.05 LAI), as was the noise resulting from a spectral band output change due to a shift in center wavelength of 2 nm (± ~0.02 LAI). The after-launch spectral-band output change resulting from a 2 nm center wavelength shift varies from 0.5 percent (bands 1 and 2) to 2 percent (bands 3 and 4) [25]. Further analysis is needed to couple all sources of error in an end-to-end (sensor to vegetation) model.

Fig. 9(b) presents the absolute error $VI_p - VI$ in each VI as a function of atmospheric and soil variations and instrument characteristics. The absolute error gives an indication of how the VI values themselves may vary as a result of various perturbances. Thus, a 5 percent radiometric uncertainty results in absolute errors of ±0.03–±0.05 VI units. This is in contrast to combined, soil and

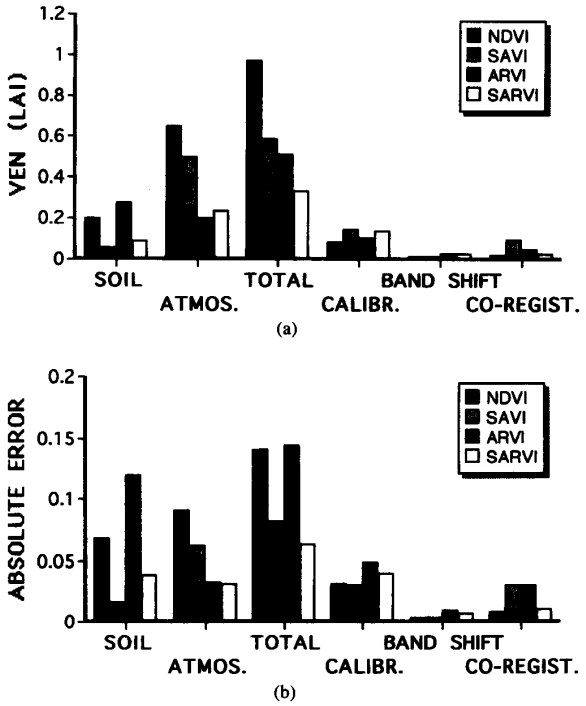

Fig. 9. Comparisons of averaged vegetation equivalent noise (a) and averaged absolute error (b) among various sources of environmental and instrument uncertainties.

atmospheric uncertainties from ±0.06 (SARVI) to ±0.14 (NDVI and ARVI) VI units.

V. Conclusions and Discussion

The goal of this study was to examine the noise and uncertainty in the NDVI equation and variants to determine if there is sufficient improvement in the new VI's to justify their global use for the EOS-MODIS sensor. The results of this study suggest that both the atmospheric and soil sources of uncertainty present in the NDVI can be markedly improved through the incorporation of soil adjusting and atmospheric correcting coefficients. These coefficients require no further information on soil and/or atmospheric conditions.

Utilizing calibrated "at sensor" radiances, one may compute the VI's based on sensor radiances normalized by incoming exoatmospheric irradiances ("apparent reflectances") or one may compute the VI's from partial or total atmospherically corrected data. Currently, a partial atmospheric correction for Rayleigh scattering and ozone absorption is used operationally in the generation of AVHRR-NDVI global data sets. These atmospheric processing scenarios affect the optimal VI equation, such that

1) if there was a total atmospheric correction then there would mainly be "soil noise" and the SAVI and MSAVI would be the best equation to use and the NDVI and ARVI would be the worst;
2) if there was a partial atmospheric correction to re-

move the Rayleigh and ozone components, then the best VI's to use would be the SARVI and MSARVI, with the NDVI and ARVI being the worst; and

3) if there was no atmospheric correction at all, i.e., no Rayleigh, ozone, or aerosol correction, then the SARVI would become slightly worse but still would have the least overall noise. The NDVI and ARVI would have the most noise and error.

With a complete, operational correction for atmospheric effects (aerosols and gases) [26], all VI's could be computed from "surface reflectance" inputs although, with atmospheric influences removed, there may no longer be a need for the atmospherically resistant variants ARVI, SARVI, and MSARVI. Nevertheless, as it may not be possible to implement a globally consistent, atmospheric correction scheme, e.g., the dark object subtraction method, there may be areas in which only a Rayleigh correction can be made or possibly, only a first-order correction based on climatology. This presents justification to maintain some resistance to atmospheric influences in the index itself, as the quality of the correction may vary greatly and affect the integrity and quality of the VI global data base.

Although the resulting new and improved indexes markedly minimized soil or atmospheric influences, they were not both reduced in a systematic, predictable manner. Atmospheric noise was found to vary with the type of soil background and soil noise was found to be a function of atmospheric condition. A feedback problem was evident whereby the improvement of one form of noise increased the other forms of noise. It may be necessary to further explore and adjust the L factor in the SAVI equation and the gamma term in the SARVI/ARVI equations to find ways to optimize normalization of soil and atmospheric influences over a wide range of land cover situations. The combined soil–atmosphere interactive noise may also be reduced by utilizing feedback mechanisms to produce a more stable equation.

For temporal and dynamic VI analysis, other sources of error include image to image misregistration, subpixel clouds, and sun-target-sensor angular (bidirectional) considerations [27].

Acknowledgment

The authors wish to thank K. Batchily for his assistance and help with the SAIL model simulations. This project was supported by MODIS contract NAS5-31364.

References

[1] C. J. Tucker and P. J. Sellers, "Satellite remote sensing of primary productivity," *Int. J. Remote Sens.*, vol. 7, pp. 1395–1416, 1986.

[2] C. O. Justice, J. R. G. Townshend, B. N. Holben, and C. J. Tucker, "Analysis of the phenology of global vegetation using meteorological satellite data," *Int. J. Remote Sens.*, vol. 6, pp. 1271–1318, 1985.

[3] S. W. Running, "Estimating terrestrial primary productivity by combining remote sensing and ecosystem simulation," *Ecological Studies, vol. 79, Remote Sensing of Biosphere Functioning*, H. Mooney and R. Hobbs., Eds. New York: Springer-Verlag, 1990, pp. 65–86.

[4] J. T. Townshend, C. Justice, W. Li, C. Gurney, and J. McManus, "Global land cover classification by remote sensing: Present capabilities and future capabilities," *Remote Sens Environ.*, vol. 35, pp. 243–255, 1991.

[5] S. N. Goward and K. E. Huemmerich, "Vegetation canopy PAR absorptance and the normalized difference vegetation index: An assessment using SAIL model," *Remote Sens. Environ.*, vol. 39, pp. 119–140, 1992.

[6] G. Asrar, M. Fuchs, E. T. Kanemasu, and J. L. Hatfield, "Estimating absorbed photosynthetic radiation and leaf area index from spectral reflectance in wheat," *Agron. J.*, vol. 76, pp. 300–306, 1984.

[7] B. J. Choudhury, "Relationships between vegetation indices, radiation absorption, and net photosynthesis evaluated by a sensitivity analysis," *Remote Sens. Environ.*, vol. 22, pp. 209–233, 1987.

[8] P. J. Sellers, "Canopy reflectance, photosynthesis and transpiration," *Int. J. Remote Sens.*, vol. 6, pp. 1335–1372, 1985.

[9] R. D. Jackson and P. J. Pinter, Jr., "Spectral response of architecturally different wheat canopies," *Remote Sens. Environ.*, vol. 20, pp. 43–56, 1986.

[10] R. B. Myneni, G. Asrar, D. Tanre, and B. J. Choudhury, "Remote sensing of solar radiation absorbed and reflected by vegetated land surfaces," *IEEE Trans. Geosci. Remote Sens.*, vol. 30, pp. 302–314, 1992.

[11] R. D. Jackson and A. R. Huete, "Interpreting vegetation indices," *Prev. Vet. Med.*, vol. 11, pp. 185–200, 1991.

[12] A. R. Huete, "A soil adjusted vegetation index (SAVI)," *Remote Sens. Environ.*, vol. 25, pp. 295–309, 1988.

[13] W. Bausch, "Soil background effects on reflectance-based crop coefficients for corn," *Remote Sens. Environ.*, vol. 46, pp. 1–10, 1993.

[14] J. Qi, A. R. Huete, M. S. Moran, A. Chehbouni, and R. D. Jackson, "Interpretation of vegetation indices derived from multi-temporal SPOT images," *Remote Sens. Environ.*, vol. 44, pp. 89–101, 1993.

[15] A. R. Huete, G. Hua, J. Qi, A. Chehbouni, and W. J. D. G. van Leeuwen, "Normalization of multidirectional red and NIR reflectances with the SAVI," *Remote Sens. Environ.*, vol. 40, pp. 1–20, 1992.

[16] F. Baret, G. Guyot, and D. Major, "TSAVI: A vegetation index which minimizes soil brightness effects on LAI and APAR estimation," in *Proc. 12th Canad. Symp. Remote Sens. IGARSS'90*, Vancouver, B.C. Canada, July 10–14, 1989.

[17] J. Qi, A. Chehbouni, A. R. Huete, Y. H. Kerr, and S. Sorooshian, "A modified soil adjusted vegetation index," *Remote Sens. Environ.*, vol. 47, 1994.

[18] Y. J. Kaufman and D. Tanre, "Atmospherically resistant vegetation index (ARVI) for EOS-MODIS," *IEEE Trans. Geosci. Remote Sens.*, vol. 30, pp. 261–270, 1992.

[19] R. B. Myneni and G. Asrar, "Atmospheric effects and spectral vegetation indices," *Remote Sens. Environ.*, vol. 47, pp. 390–402, 1994.

[20] V. V. Salomonson, W. L. Barnes, P. W. Maymon, H. E. Montgomery, and H. Ostrow, "MODIS: Advanced facility instrument for studies of the earth as a system," *IEEE Trans. Geosci. Remote Sens.*, vol. 27, pp. 145–153, 1989.

[21] S. W. Running, C. Justice, V. Salomonson, D. Hall, J. Barker, Y. Kaufman, A. Strahler, A. Huete, J. Muller, V. Vanderbilt, Z. Wan, P. Teillet, and D. Carneggie, "Terrestrial remote sensing science and algorithms planned for EOS/MODIS," *Int. J. Remote Sens.*, vol. 15, 1994.

[22] W. Verhoef, "Light scattering by leaf layers with application to canopy reflectance modelling: The SAIL model," *Remote Sens. Environ.*, vol. 16, pp. 125–141, 1984.

[23] F. X. Kneizys, E. P. Shettle, L. W. Abreu, J. H. Chetwynd, G. P. Anderson, W. O. Gallery, J. E. A. Selby, and S. A. Clough, "User's guide to LOWTRAN 7," AFRCL, Bedford, MA, Rep. AFGL-TR-88-0177, 137 pp., Aug. 1988.

[24] A. R. Huete, C. Justice, and H. Liu, "Development of vegetation and soil indices for MODIS-EOS," *Remote Sens. Environ.*, vol. 48, pp. 1–11, 1994.

[25] J. L. Barker, K. S. Brown, J. M. K. Harnden, P. Anuta, P. Ardanuy, T. Bryant, G. Kvaran, E. Knight, A. McKay, and J. Smid, "MODIS calibration & characterization algorithm theoretical basis document (CAL ATBD)," version 0, personal communication, July 1993.

[26] M. D. King, Y. J. Kaufman, W. P. Menzel, and D. Tanre, "Remote sensing of cloud, aerosol, and water vapor properties from the moderate resolution imaging spectrometer (MODIS)," *IEEE Trans. Geosci. Remote Sens.*, vol. 30, pp. 2–27, 1992.

[27] J. T. Townshend, C. Justice, C. Gurney, and J. McManus, "The impact of misregistration on the detection of changes in land cover," *IEEE Trans. Geosci. Remote Sens.*, 1992.

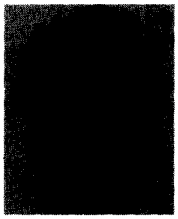

Alfredo R. Huete received the M.S. degree in plant and soil biology from the University of California, Berkeley, in 1982, and the Ph.D. degree in soil and water science from the University of Arizona, Tucson, 1984.

He is presently an Associate Professor with the Department of Soil and Water Science, University of Arizona, and heads the Laboratory for Terrestrial Physics program. He received NASA Faculty Fellowship Awards, for summer 1987 and summer 1988 and is now on the MODIS Science Team developing soil and vegetation indexes, leaf area index, and land cover algorithms. His research interests include the global study of vegetation dynamics and their interactions with soil and climate.

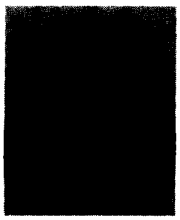

Hui Qing Lui received the B.S. degree in electronic engineering from Harbin Institute of Technology, People's Republic of China in 1982, and the M.S. degree in Agrisystems and biosystems engineering from the University of Arizona, Tucson, in 1992.

Since 1992, she has been with the Laboratory for Terrestrial Physics as a Senior Research Specialist. She is working on experimental and simulation data generation for remote sensing studies of vegetation, soil, and the atmosphere. She is conducting error and sensitivity analyses for the vegetation index satellite algorithms for MODIS as well as managing the Science Computing Facility.